Influence of rare-earth impurities on the Ge and Ga local structure in the $Ca_3Ga_2Ge_3O_{12}$ glass

Agnieszka Witkowska [a,b,*], Bohdan Padlyak [c,d], Jaroslaw Rybicki [a,b]

[a] *Department of Solid State Physics, Faculty of Technical Physics and Applied Mathematics, Gdansk University of Technology, Narutowicza 11/12, 80-952 Gdansk, Poland*
[b] *TASK Computer Centre, Narutowicza 11/12, 80-952 Gdansk, Poland*
[c] *Department of Physics, Kazimierz Wielki University of Bydgoszcz, Weyssenhoff Sq. 11, 85-072 Bydgoszcz, Poland*
[d] *Institute of Physical Optics, Dragomanov St. 23, 79-005 Lviv, Ukraine*

Available online 12 September 2006

Abstract

The present contribution presents X-ray absorption fine structure (XAFS) measurements and analysis of the Ge and Ga local structure in glass of $Ca_3Ga_2Ge_3O_{12}$ composition, doped with rare-earth metals (Ce, Eu, Ho, Er in the amount of 0.7 wt% and Nd in the amount of 1.0 wt%). The Ge and Ga ion neighborhoods in the considered glass samples have been compared with data obtained for undoped glass. The results have shown that introduction of rare-earth ions modifies the local structure around the Ga ions in the glass network, leaving the same occurrence ratio of the GaO_4 and GaO_6 structural units as in undoped $Ca_3Ga_2Ge_3O_{12}$ glass. At the same time, the GeO_2 subsystem remains completely unaffected by the presence of rare-earth dopants.
© 2006 Elsevier B.V. All rights reserved.

PACS: 61.43.–j; 61.10.Ht

Keywords: Disordered solids; XAFS

1. Introduction

Disordered crystals and glass matrices doped with transition and rare-earth metals' ions are very attractive as possible laser media (especially for tunable solid state lasers), optical fibers and for other applications in optoelectronics [1–3]. Experimental investigations and theoretical analysis of spectroscopic properties of transition and rare-earth impurity metal ions in disordered compounds, particularly compositionally (or substitutionally) disordered oxide crystals and glasses, are current topics of solid state physics and optical materials technology. This also concerns CaO–Ga_2O_3–GeO_2 compounds, which can be obtained in crystalline and glassy states. These compounds are novel

materials for quantum electronics and other applications. In particular, CaO–Ga_2O_3–GeO_2 glasses are promising materials for red phosphors (when activated with Eu^{3+}) and green lasers, as well as IR LED pumping up-converted lasers, operating in the visible spectral region (when activated with Ho^{3+} and Er^{3+} ions).

Electron paramagnetic resonance (EPR) and optical spectroscopy are powerful methods to study the local environment and crystal field parameters for dopant ions in single crystals. However, interpretation of EPR and optical spectra of rare-earth metal ions in glasses requires a detailed structural investigation of glasses and comparison of the obtained results with well-known structural data for their crystalline analogues. Therefore, a detailed structural study of CaO–Ga_2O_3–GeO_2 glasses is necessary (local neighborhoods of Ga or Ge and of impurity ions). The extended X-ray absorption fine structure (EXAFS) method is characterized by atomic selectivity and high sensitivity to the short-range order, and it thus appears to be the most

---

* Corresponding author. Address: Department of Solid State Physics, Faculty of Technical Physics and Applied Mathematics, Gdansk University of Technology, Narutowicza 11/12, 80-952 Gdansk, Poland.
E-mail address: agnieszka@mif.pg.gda.pl (A. Witkowska).

suitable technique to study atom neighborhoods in multi-component and disordered systems, particularly in the case of very low photoabsorber concentrations.

Earlier studies of the $Ca_3Ga_2Ge_3O_{12}$ glass by X-ray scattering and molecular dynamics simulations have shown that their structure is characterized by a short-range ordering similar to that of the corresponding crystalline compounds and that their glass network is built of GaO_6 octahedra and $(Ga/Ge)O_4$ tetrahedra [4]. On the basis of EXAFS analysis at Ga and Ge K-edges, detailed structural parameters of the glass have been obtained and compared with the ordered $Ca_3Ga_2Ge_3O_{12}$ crystal structure [5]. It should be noted that significant redistribution of GaO_4 and GaO_6 units has been detected.

The present paper is organized as follows. Section 2 covers technical issues: the EXAFS measurements and the analysis method are described. Experimental results of the X-ray absorption fine structure (XAFS) measurements at the Ge and Ga K-edges and EXAFS analysis are presented and discussed in Section 3. Section 4 contains our concluding remarks.

2. Technical issues

2.1. EXAFS measurements

Ce-, Nd-, Eu-, Ho- and Er-doped glass samples of high chemical purity and optical quality of $Ca_3Ga_2Ge_3O_{12}$ general composition were obtained in corundum crucibles with the conventional high-temperature synthesis technique (for detail see [6]). The europium impurity was added to the glass composition as $EuCl_3$ liquid solution in the amount of 0.7 wt%. The holmium, erbium and cerium impurities were respectively added as Ho_2O_3, Er_2O_3 and Ce_2O_3 powdered compounds, in the amounts of 0.7 wt%. Neodymium was added to the glass composition as Nd_2O_3 in the amount of 1.0 wt%. The chemical composition of the obtained samples was controlled with the X-ray microanalysis technique using a 'Camebax' apparatus. The Eu- and Ho-doped glasses were characterized by light yellow color, while the Er- and Nd-doped glasses were respectively light pink and light blue in color. The Ce-doped glass was characterized by intense yellow color. Powdered samples as well as bulk samples were used for the X-ray scattering measurements, the latter with the approximate size of $8 \times 4 \times 3$ mm³. The doped glasses have exhibited typical glassy-like X-ray structure factors, quite similar to the structure factor of undoped glass of the same composition [4].

Finally, the glasses were milled (to the grain diameter of about 1 µm) and the powder so obtained was used to prepare pellets for XAFS measurements. 20 mg of powder was carefully mixed with 180 mg BN and pressed, thus producing homogenous pellets 12 mm in diameter, and 2–3 mm thick.

The spectra of doped $Ca_3Ga_2Ge_3O_{12}$ glasses at the Ge and Ga K-edges were recorded at the A1 beamline station at HASYLAB, Hamburg. Room temperature measurements were performed in the 10.8–12.1 keV and 10.1–11.0 keV energy ranges for the Ge K-edge (11.104 keV) and the Ga K-edge (10.367 keV), respectively. The sampling procedure was so chosen as to yield high quality data for both pre- and post-edge background analyses used to normalize the spectra. Further detail of the experimental setup can be found in [7].

2.2. Analysis method

The experimental data were analyzed with an advanced technique using theoretical calculations of the X-ray absorption cross-section in the framework of the GNXAS method [8–11] (GN stands for the *n*-atom distribution function in condensed matter, g_n, XAS denotes X-ray absorption spectroscopy). The main characteristic of the method is the possibility to calculate and perform the configurational average of multiple-scattering (MS) contributions (at any order) associated with two-, three- and four-atom configurations, $\gamma^{(2)}$, $\gamma^{(3)}$ and $\gamma^{(4)}$ signal, respectively. This is accomplished by a continued fraction expansion algorithm [8]. In our analysis only the two-body term, $\gamma^{(2)}$, was used. Other signals, associated with e.g., three-body configurations, were beyond the sensitivity of the EXAFS method in the case of the considered materials. Calculation of the XAS $\gamma^{(2)}$ signal was performed using an accurate complex energy-dependent self-energy function, which automatically accounts for the inelastic mean-free-path (MFP) of the excited photoelectron and for the core-hole lifetime.

In addition, the GNXAS scheme can account for multi-electron excitation channels, affecting the modelling of the post-edge atomic backgrounds. Inaccurate extraction of the atomic background neglecting double-electron channels may result in the presence of low-frequency components without structural origin in the EXAFS signal.

Finally, the GNXAS method is based on comparison in the energy space between the experimental EXAFS signal and the theoretical one, composed of an appropriate background and the structural oscillation calculated for a chosen structural model, in an attempt to optimize the value of relevant structural parameters (describing the short-range ordering around a selected atomic site) and non-structural parameters (e.g., experimental resolution, S_0^2, E_0).

As a simple Gaussian shape of the short-range peak of a pPDF (partial pair distribution function) is usually insufficient to describe accurately the short-range ordering of highly disordered systems, the bond length probability density, $p(r)$, was modelled using a Γ-like distribution [9]:

$$p(r) = \frac{2N_c}{\sigma|\beta|\Gamma(\frac{4}{\beta^2})} \left[\frac{4}{\beta^2} + \frac{2(r-R)}{\beta\sigma} \right]^{\left(\frac{4}{\beta^2}-1\right)}$$
$$\times \exp\left[-\left(\frac{4}{\beta^2} + \frac{2(r-R)}{\beta\sigma} \right) \right], \tag{1}$$

defined for $(r - R)\beta > -2\sigma$. In Eq. (1) $\Gamma(\cdot)$ is the Euler Gamma function, while N_c is the coordination number, R – the average inter-atomic distance, σ – the standard deviation of distance, and β – the skewness parameter.

The most important non-structural parameter is S_0^2, the amplitude reduction factor, accounting for effective many-body correction to the one-electron cross-section. For all the considered glasses S_0^2 was in the (0.75–0.8) range. Another parameter, E_0, describing the shift between experimental and theoretical energy scales, reached a value about 5 eV higher than the edge energy taken as the maximum of the spectrum derivative calculated near the threshold.

3. Results and discussion

In this Section the results of structural analysis performed according to the above mentioned methods are presented. The analysis has been focussed on the short-range (oxide) ordering around Ge and Ga ions of the considered structures doped with ions of rare-earth metals. The structural parameters of the other two-body correlations, Ge–Ga, Ge–Ca, Ga–Ca and Ga–Ge, have also been obtained, but the uncertainties of determination of these parameters are so great, that our discussion will be qualitative rather than quantitative.

As our analysis of the spectra's shape near the absorption edge (XANES region – X-ray absorption near edge structure) had shown no significant differences among the various compositions of the examined material, they were analyzed in the EXAFS range.

In our GNXAS analysis of the Ge and Ga K-edge spectra the following three-shell frequency contribution was taken into account in modelling the theoretical signal: Ge–O, Ge–Ca and Ge–Ga for the Ge-edge spectra, and Ga–O, Ga–Ca and Ga–Ge for the Ga-edge spectra. Components of the model signals and quality of the fitting procedure are shown, for example, in the case of Eu-doped glass in Fig. 1(a) and (b) (for the Ge and the Ga K-edge, respectively). The post-edge background was modelled piece-wise by spline functions of the third and fourth degree, taking into account double-electron excitation channels such as (1s 3s) and (1s 3p).

The influence of various contents of rare-earth metals' ions in the $Ca_3Ga_2Ge_3O_{12}$ glassy matrix on the Ge local structure is shown in Fig. 2. No significant correlation between the type of rare-earth impurity and the shape of the EXAFS signal has been detected. Detailed structural parameters of the Ge–O distribution are presented in Table 1. The accuracy of the mean distance between the photoabsorber and the nearest neighbor amounts to 0.01 Å. Parameters σ^2 and N have been determined with an error of about 10%. The accuracy of β determination has been about 30%.

The contents of Table 1 suggests that, independently of the rare-earth ion's type, the Ge local structure is characterized by $R = 1.75(1)$ Å, $\sigma^2 = 0.0020(2)$ Å^2, $\beta = 0.3(1)$ and $N = 4.0(3)$. This means that, like in crystalline $Ca_3Ga_2Ge_3O_{12}$ or in undoped glass, structural units of the germanium oxide subsystem have the form of regular tetrahedra. Furthermore, the mean Ge–O bond length in doped glasses determined in EXAFS analysis is comparable with that determined for the undoped glass (using EXAFS, X-ray
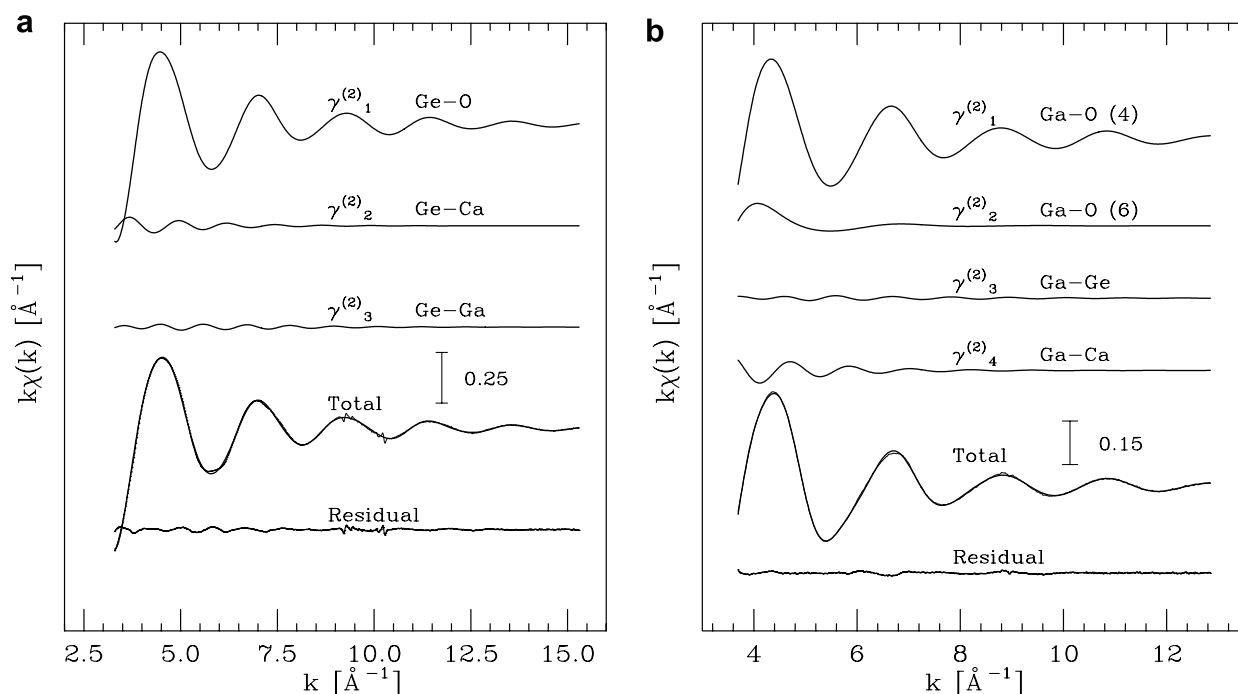

Fig. 1. Results of GNXAS analysis in $Ca_3Ga_2Ge_3O_{12}$ glass doped with 0.7 wt%. Eu ions: (a) Ge K-edge; (b) Ga K-edge. The upper curves are components of the model signal. The thick line is the model, the thin one shows the experimental results.
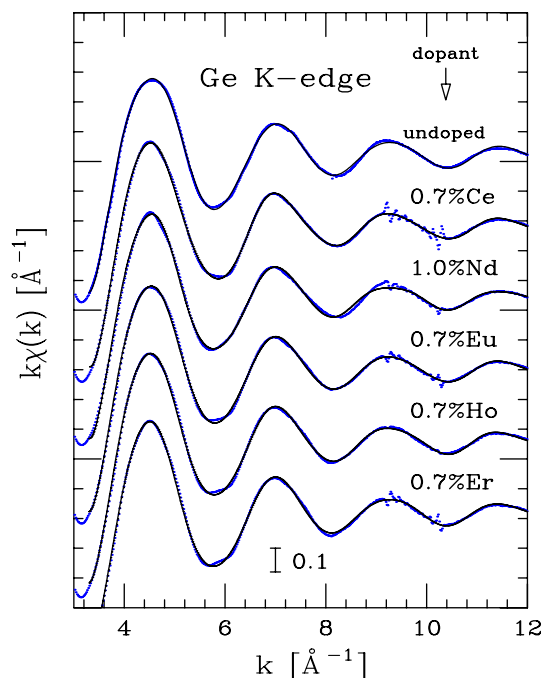
Fig. 2. Results of the Ge local neighborhood analysis obtained by the GNXAS method realized for $Ca_3Ga_2Ge_3O_{12}$ glass doped with ions of rare-earth metals. The thick line is the model, the thin one shows the experimental results.

Fig. 3. Results of Ga local neighborhood analysis obtained by the GNXAS method for $Ca_3Ga_2Ge_3O_{12}$ glass doped with ions of rare-earth metals. The thick line is the model, the thin one shows the experimental results.

Table 1
Parameters of the Ge-O correlation obtained during GNXAS analysis performed for EXAFS spectra recorded at the Ge K-edge for $Ca_3Ga_2Ge_3O_{12}$ glass doped with ions of rare-earth metals

Dopant	R (Å)	σ^2 (Å^2)	β	N
Undoped	1.75(1)	0.0016(2)	0.5(1)	3.9(3)
0.7% Ce	1.75(1)	0.0021(2)	0.3(1)	4.1(3)
1.0% Nd	1.76(1)	0.0019(2)	0.4(1)	3.9(3)
0.7% Eu	1.75(1)	0.0021(2)	0.2(1)	4.1(3)
0.7% Ho	1.75(1)	0.0020(2)	0.3(1)	4.1(3)
0.7% Er	1.76(1)	0.0021(2)	0.4(1)	4.1(3)

Results for the undoped glass taken from [5].

scattering methods and MD simulations [4,5]), and greater by as much as 0.1 Å when compared with the crystalline equivalent.

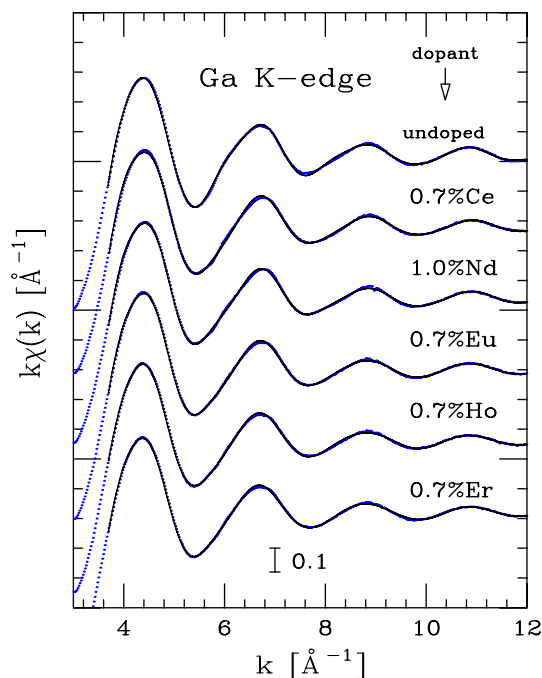The structure of Ge ion's second- and third-coordination shell in considered glasses were analyzed as well. In the course of this analysis, a small increase in mean Ge–Ca and Ge–Ga distances was observed with increasing ionic radius of the dopant. The greatest observed difference between undoped glass and that doped with 0.7 wt% of Er amounted to about 0.1 Å. The other parameters remain the same as those for the undoped glass and practically independent of the kind of dopant, subject to the limitations of the method's accuracy. Notably, the coordination number is like that of the crystalline structure, in all cases about 2.0 for Ge–Ca and 4.0 for Ge–Ga correlations.

The fitting results of the Ga K-edge analysis are shown in Fig. 3. Table 2 presents parameters of the Ga–O correlation only (with same accuracy as in the case of the Ge K-edge analysis), where two forms of structural units have been considered (as observed in crystalline and undoped glass of the $Ca_3Ga_2Ge_3O_{12}$ stoichiometry): GaO_4 tetrahedra and GaO_6 octahedra.

Analysis of the component signals obtained for GaO_4 and GaO_6 components (see e.g., components Ga–O(4)

Table 2
Parameters of the Ga–O correlation obtained during GNXAS perfomed for EXAFS spectra recorded at the Ga K-edge for $Ca_3Ga_2Ge_3O_{12}$ glass doped with ions of rare-earth metals: index 1 – units in the form of tetrahedra, index 2 – units in the form of octahedra

x	R_1 (Å)	σ_1^2 (Å^2)	β_1	N_1	R_2 (Å)	σ_2^2 (Å^2)	β_2	N_2
Undoped	1.87(1)	0.0039(4)	1.3(4)	3.8(3)	2.29(2)	0.10(1)	1.2(4)	6.0(6)
0.7% Ce	1.86(1)	0.0034(3)	0.8(2)	3.6(3)	2.25(2)	0.12(1)	1.0(3)	6.1(6)
1.0% Nd	1.86(1)	0.0035(4)	0.9(3)	3.5(3)	2.18(2)	0.12(1)	0.9(3)	6.0(6)
0.7% Eu	1.86(1)	0.0031(3)	0.8(2)	3.3(3)	2.19(2)	0.12(1)	1.0(3)	6.0(6)
0.7% Ho	1.86(1)	0.0036(4)	0.8(2)	3.3(3)	2.20(2)	0.12(1)	1.0(3)	6.1(6)
0.7% Er	1.86(1)	0.0033(3)	0.8(2)	3.0(3)	2.17(2)	0.08(1)	1.0(3)	6.0(6)

Results for the undoped glass taken from [5].

and Ga–O(6), respectively, in Fig. 1(b) suggests that doping with ions of rare-earth metals in amounts about of 0.7 wt% does not cause redistribution of the GaO_4 and GaO_6 structural units in relation to the undoped $Ca_3Ga_2Ge_3O_{12}$ glass. Still, GaO_4 units dominate and are more regular than the GaO_6 groups (compare σ^2 and β-parameters). However, we observe significant changes in the structure of the gallium oxide subsystem. Firstly, in the case of the tetrahedral form, an increase in the dopant's ionic radius induces a decrease of the coordination number (from about 4.0 to about 3.0). Secondly, in the case of the octahedral form, the average Ge–O distance decreases as a result of incorporation of the rare-earth metal ions.

Some changes have also been observed in the Ga–Ca two-body correlation: decreased mean distance between the photoabsorber and the neighbor, decreased mean number of calcium around gallium (by more than 1.0), and decreased distribution asymmetry (β-parameters).

4. Conclusions

EXAFS study results of the Ge and Ga local structure in the $Ca_3Ga_2Ge_3O_{12}$ glass doped with rare-earth metals (Ce, Nd, Eu, Ho, Er) have been presented above. Their analysis on the basis of the GNXAS approach indicates that introduction of rare-earth ions into a $Ca_3Ga_2Ge_3O_{12}$ glass matrix may alter its structure around the Ga only, while the GaO_4/GaO_6 ratio and regularity of units remain unchanged. The local structure around germanium remains exactly the same as in undoped glass and is still more ordered than that of gallium.

However, to gain deeper insight into the glass structure modification related to impurity ions' presence, a local environment study of rare-earth metals in doped glasses is necessary. This is the subject of our forthcoming work.

Acknowledgments

References

[1] J. Drube, B. Struve, G. Huber, Opt. Commun. 50 (1984) 45.
[2] P. Kenyon, L. Andrews, B. Mc Collum, A. Lempicki, IEEE Quantum Electron. 18 (1982) 1189.
[3] D.C. Yeh, W.A. Sibley, M. Suscavage, M.G. Drexhange, J. Appl. Phys. 62 (1987) 266.
[4] B. Padlyak, S. Mudry, V. Halchak, A. Korolyshyn, J. Rybicki, A. Witkowska, Opt. Appl. 30 (4) (2000) 691.
[5] D. Chelstowski, A. Witkowska, J. Rybicki, B. Padlyak, A. Trapananti, E. Principi, Opt. Appl. 33 (1) (2003) 125.
[6] B. Padlyak, P.P. Buchynskii, Patent of Ukraine No. UA 25235 A, October 30, 1998.
[7] http://www-hasylab.desy.de/.
[8] A. Filipponi, A. Di Cicco, Phys. Rev. B 51 (1995) 12322.
[9] A. Filipponi, A. Di Cicco, C.R. Natoli, Phys. Rev. B 52 (1995) 15122; A. Filipponi, A. Di Cicco, C.R. Natoli, Phys. Rev. B 52 (1995) 15135.
[10] A. Filipponi, A. Di Cicco, TASK Quart. 4 (2000) 575.
[11] http://gnxas.unicam.it.